Published in final edited form as:
J Cardiovasc Pharmacol. 2014 June ; 63(6): 533–543. doi:10.1097/FJC.0000000000000078.

PP2 Prevents Isoproterenol Stimulation of Cardiac Pacemaker Activity

Jianying Huang, PhD[1,2,#], **Yen-Chang Lin, PhD**[3], **Stan Hileman, PhD**[2], **Karen H Martin, PhD**[4,5], **Robert Hull, MD**[6], and **Han-Gang Yu, PhD**[1,2]

[1]Center for Cardiovascular and Respiratory Sciences, West Virginia University, Morgantown, WV 26506

[2]Department of Physiology and Pharmacology, West Virginia University, Morgantown, WV 26506

[3]Graduate Institute of Biotechnology, Chinese Culture University, Taiwan

[4]Mary Babb Randolph Cancer Center, West Virginia University, Morgantown, WV 26506

[5]Department of Neurobiology and Anatomy, West Virginia University, Morgantown, WV 26506

[6]Heart Institute of Health Sciences Center, West Virginia University, Morgantown, WV 26506

Abstract

Increasing evidence has demonstrated the potential risks of cardiac arrhythmias (such as prolonged QT interval) using tyrosine kinase inhibitors for cancer therapy. We report here that a widely used selective inhibitor of Src tyrosine kinases, PP2, can inhibit and prevent isoproterenol stimulation of cardiac pacemaker activity. In dissected rat sinus node PP2 inhibited and prevented isoproterenol stimulation of spontaneous beating rate. In isolated sinus node myocytes PP2 suppressed the hyperpolarization-activated "funny" current (I_f) by negatively shifting the activation curve and decelerating activation kinetics, associated with decreased cell surface expression and reduced tyrosine phosphorylation of hyperpolarization-activated, cyclic nucleotide-modulated channel 4 (HCN4) channel proteins. In human embryonic kidney 293 cells overexpressing recombinant human HCN4 channels, PP2 reversed isoproterenol stimulation of HCN4 and inhibited HCN4-573x, a cAMP insensitive human HCN4 mutant. Isoprotenrenol had little effects on HCN4-573x. These results demonstrated that inhibition of presumably tyrosine Src kinase activity in heart by PP2 decreased and prevented the potential β-adrenergic stimulation of cardiac pacemaker activity. These effects are mediated, at least partially, by a cAMP-independent attenuation of channel activity and cell surface expression of HCN4, the key channel protein that controls the heart rate.

Corresponding author: Han-Gang Yu, Center for Cardiovascular and Respiratory Sciences, Department of Physiology and Pharmacology, West Virginia University, Morgantown, WV 26506, Tel: 304-293-2324, Fax: 304-293-5513, hyu@hsc.wvu.edu.
[#]Current affiliation: [a]Department of Neurology and [b]Center for Neuroscience and Regeneration Research, Yale University School of Medicine, New Haven, CT 06510, [c]Rehabilitation Research Center, Veterans Affairs Connecticut Healthcare System, West Haven, CT 06516

Keywords

PP2; isoproterenol; Src tyrosine kinases; tyrosine phosphorylation; pacemaker current I_f; HCN4; sinus node

INTRODUCTION

Tyrosine kinases are important in cell physiology such as cell division and angiogenesis and are targets for cancer therapy (1). The non-receptor tyrosine kinase Src is essential in cell functions (2). Src was also the first tyrosine kinase to be identified in promotion of tumor growth (2, 3). Src protein levels are often overexpressed in cancers (3). Thus, inhibition of Src tyrosine kinase activity represents a main strategy in cancer therapy (4). PP2 is a widely used selective inhibitor for Src tyrosine kinases (STK) (5–7) and has been targeted to develop as an anti-cancer drug (8, 9).

The well-established adrenergic signaling pathway that mediates the regulation of heart rate is through β-adrenergic receptor activation, G-protein, adenylate cyclase, and cAMP (10, 11). Stimulation of β-adrenergic receptors by β agonist, isoproterenol (ISO) increases the intracellular cAMP concentration (11). cAMP increases I_f by shifting its voltage-dependent activation toward more positive potentials associated with acceleration of activation kinetics (11). Activated near the end of sinus node repolarization, I_f is an important contributor to the early diastolic depolarization (11). The amplitude and speed of I_f activation determine the slope of early diastolic depolarization, which determines the sinus node pacemaker activity and thus, the heart rate (11).

I_f is generated by HCN channels. Three isoforms (HCN1, HCN2, HCN4) are present in the heart with HCN4 being the prevalent isoform in the sinus node (12). HCN4 gating is internally inhibited by a C-linker located in the beginning of the C-terminus (13). cAMP acts on HCN4 by directly binding to the cyclic nucleotide binding domain (CNBD) in the C-terminus, which releases the C-linker inhibition on the channel gating, leading to faster opening at more positive potentials (13). Therefore, cAMP sensitivity of HCN4 has been proposed as a key event for control of heart rate (14).

Our previous studies have indicated a positive correlation of tyrosine phosphorylation with the HCN4 channel activity (15–17). Increased STK activity increases HCN4 activity associated with an enhanced surface expression and tyrosine phosphorylation of the channel protein, whereas inhibited STK activity by PP2 decreases HCN4 channel conductance associated with a decreased tyrosine phosphorylation of the channel proteins. In addition, we and others have identified the sites that mediate Src modulation of HCN channels (5, 18).

In this work, we focused on contribution of HCN4 to the potential PP2-induced inhibition of β-adrenergic stimulation of cardiac pacemaker activity, possibly via a mechanism independent of cAMP.

METHODS

Original studies reported here have been carried out in accordance with the Declaration of Helsinki and/or with the Guide for the Care and Use of Laboratory Animals as adopted and promulgated by the U.S. National Institutes of Health. The animal protocols were reviewed and approved by our university animal care and use committee.

Dissection of rat sinus node and isolation of sinus node myocytes

The heart was quickly removed from anesthetized adult Sprague-Dawley rat with sodium pentobarbital (100 mg/kg) and immersed in normal Tyrode solution containing heparin. The sinoatrial region was dissected and placed in Tyrode gassed with 100% O_2 at 37°C. We used a modified method to identify and isolate rat sinus node myocytes (19). Briefly, the sinoatrial region was digested in a Ca^{2+}-free Tyrode solution containing 0.4mg/ml Librase Blendyme 4 (Roche Applied Sciences) for approximately 20 min at 37°C. After digestion, the tissue was trimmed into strips of ~1mm in width and 3–4 mm in length in Ca^{2+} -free Tyrode solution. The digested tissue was then placed in Krafte-brühe (KB) solution. The sinus node myocytes were dissociated by gently puffing KB solution onto the tissue. Normal Tyrode solution contained (mM): NaCl, 140; KCl, 5.4; $CaCl_2$, 1.8; $MgCl_2$, 1; D-Glucose, 5.5; HEPES-NaOH, 5; pH 7.4. Krafte-brühe (KB) solution contained (mM): L-glutamic acid 50, KOH 80, KCl 40, $MgSO_4$ 3, KH_2PO_4 25, HEPES 10, EGTA 1, taurine 20 and glucose 10; pH 7.2.

Figure S1 shows the morphology of rat sinus node (A) and myocytes isolated from it (B). Typical spindle-like or elongated spindle-like sinus node myocytes are shown in a–d. An atrial myocyte is also shown on the right for comparison (e). Regardless of different types of cells, we only selected cells with spontaneous action potentials (C) for patch clamp studies.

Immunofluorescence imaging of single sinus node myocytes

Isolated sinus node myocytes were placed on glass slides, and left to settle for at least 1 hour before fixation in 4% paraformaldehyde (PFA) for 20 min at room temperature. For drug treatments, a final concentration of 10 μM PP3, 10 μM PP2, or 100 nM of ISO in phosphate buffered saline (PBS) were incubated with semi-adhered myocytes for 10 min. PFA was removed and myocytes were washed for three times with PBS. The cells were then permeablized with 0.5% Triton-X 100 in PBS for 2 min and rinsed with PBS for three times. Then the cells were blocked for 30 min at room temperature using PBS containing 2% BSA. Primary antibodies against HCN4 (Abcam) and phosphotyrosine (4G10, Millipore) were prepared by 1:100 dilution in the blocking solution, in which the cells were incubated over two nights at 4°C. After three times of washes with PBS, the secondary antibodies (1:1000, Alexa Fluor 488 and 555, Invitrogen) were added and incubated for 1 hr in the dark at room temperature. Following the final rinses with PBS and subsequently distilled water, the glass slides were coverslipped using 10μl Prolong Gold with DAPI (Invitrogen). This mounting media requires curing overnight in the dark at room temperature. The slides were then ready for examination using confocal laser scanning LSM510 microscopy (Carl Zeiss). All imaging experiments were performed at room temperature.

Quantification of fluorescence signal for surface and intracellular HCN4 channels

After background fluorescence subtraction, the surface expression of HCN4 is identified from fluorescence in the peripheral plasma membrane, confirmed with a membrane marker, DiL (Invitrogen), by colocalization. Image analysis was performed by LSM510, and quantification of fluorescent signal by ImageJ (NIH). Intracellular fluorescence was obtained by subtracting the total cell fluorescence by fluorescence on the peripheral plasma membrane.

Whole-cell patch clamp studies of I_f and I_{HCN4}

Whole-cell patch clamp technique was used to study I_f in myocytes isolated from rat sinus node at 33±1°C and HCN4 and 573x expressed in HEK293 cells at room temperature (25±1°C).

Sinus node action potential and I_f currents were recorded at 33 ± 1°C using either the whole-cell or the amphotericin-B perforated patch clamp to avoid I_f rundown (20). Amphotericin - B was added to the internal solution to a final concentration of 240 μg/ml on the day of use. Action potentials were recorded in normal Tyrode containing (mM): NaCl 140, KCl 5.4, $CaCl_2$ 1.8, $MgCl_2$ 1, Glucose 5.5, Hepes 5, pH 7.4 adjusted by NaOH. The pipettes had a resistance of 6–8 MΩ when filled with internal solution composed of (mM): NaCl 10, K-aspartate 130, $MgCl_2$ 2, $CaCl_2$ 2, EGTA 5, Na_2-ATP 2, GTP (sodium salt) 0.1, creatine phosphate 5, pH 7.2 by KOH.

Unless stated otherwise, for I_f recordings, potassium channel blockers (2mM 4-AP, 2mM Ba^{2+}) and calcium channel blockers (0.1mM Cd^{2+}, 2mM Mn^{2+}) were added to normal Tyrode to inhibit potassium and calcium currents, respectively, to avoid contaminating I_f deactivation at −30 mV. ATP, GTP and creatine phosphate were freshly prepared on the day of use.

For recording I_{HCN4}, day 1 up to day 3 post-transfected HEK293 cells with red fluorescence were selected for patch clamp studies. The HEK293 cells were placed in a Lucite bath with the temperature being maintained at 25 ± 1°C. I_{HCN4} currents were recorded using the whole cell patch clamp technique with an Axopatch-700B amplifier. The pipettes had a resistance of 2–4 MΩ when filled with internal solution (mM): NaCl 6, K-aspartate 130, $MgCl_2$ 2, $CaCl_2$ 5, EGTA 11, and HEPES 10; pH adjusted to 7.2 by KOH. The external solution contained (mM) NaCl 120, $MgCl_2$ 1, HEPES 5, KCl 30, $CaCl_2$ 1.8, and pH was adjusted to 7.4 by NaOH. The transient potassium current (I_{to}) blocker, 4-aminopyridine (4-AP) (2 mM), was added to the external solution to inhibit the endogenous transient potassium current, which can overlap with I_{HCN4} tail currents recorded at +40 mV.

Cell culture and plasmid transfection

HEK293 cells were grown on poly-D-lysine coated coverslips in Dulbecco's modified Eagle's medium (DMEM, Invitrogen), supplemented with 10% fetal bovine serum, 100 IU/mL penicillin, and 100 g/L streptomycin. Cells with 50–70% confluence in 6-well plates were used for plasmids transfection (1–2μg for each plasmid) using Lipofectamine2000

(Invitrogen). HCN4 and 573x plasmids were fused with GFP for verification of expression and served as a selection guidance for patch clamp studies.

Data analysis

The whole-cell patch clamp data were acquired by CLAMPEX and analyzed by CLAMPFIT (pClamp 9, Axon). Data are shown as mean ± SEM. Student's t-test and one-way ANOVA (for more than two groups) were used for statistical analysis. $P<0.05$ was considered as statistically significant.

I_f/I_{HCN4} current amplitudes were determined by measuring the time-dependent inward currents that are sensitive to blocker, 1 mM Cs^+ or 2 μM ZD7288. The activation curve was constructed on the relative membrane conductance by measuring the tail currents divided by the driving force ($E_{test} - E_{rev}$), which was then normalized to the maximal conductance. For current activation that did not reach steady-state (e.g., current traces in response to −60mV, −70mV, and −80mV pulses in Figure 3A), we fit the current traces to the steady-state using one exponential function (15) and obtained the fitted current amplitude, which was used to construct the activation curve and calculate the activation kinetics (e.g., Figs. 3B, 3C).

Drugs

Small molecule, 4-amino-5-(4-chlorophenyl)-7-(*t*-butyl)pyrazolo[3,4-d]pyrimidine (PP2), also known as AG 1897 (21), has been widely used as a selective inhibitor of Src kinases family members (9, 21). The IC_{50} of PP2 on Src kinase activity is 5–36nM (8, 9). Its inactive structural analog, 4-amino-7-phenylpyrazol[3,4-d]pyrimidine (PP3), is used as a negative control to confirm the action of PP2 (9).

RESULTS

PP2 inhibited and prevented ISO stimulation of sinus node pacemaker activity

The spontaneous beating rate of a dissected sinus node was recorded at room temperature (video S1). PP2 at 2–10 μM decreased the beating rate by 25.2 % (Figure S2, Control: 111 ± 2 bpm, PP2: 83 ± 4 bpm, $p < 0.01$, n=5). ISO at 0.1 μM increased the beating rate by 17.1% (Control: 111 ± 2 bpm, ISO: 130 ± 3 bpm, $p < 0.01$, n=5). The stimulation of ISO on the sinus node beating rate was diminished in the presence of PP2 (Control: 111 ± 2 bpm, ISO +PP2: 107 ± 4 bpm, $p = 0.4$, n=5). The sinus rate post ISO treatment was statistically significant from co-administration of ISO and PP2 ($p < 0.01$). The beating rate was not significantly affected by PP3 (Control: 111 ± 2 bpm, PP3: 109 ± 2 bpm, $p = 0.45$, n=5).

To investigate the mechanisms of PP2-induced decrease and attenuation of ISO stimulation of sinus node beating rate, we studied effects of PP2 on the action potentials in isolated sinus node myocytes. Figure 1 shows that the spontaneous action potentials in an isolated sinus node myocyte (A), were inhibited by perfusion of 2 μM PP2 for 1–2 min (B). After PP2 washout, the action potentials were partially recovered (C). ISO (10 nM) failed to speed the spontaneous action potentials in PP2-treated cells (D, E). PP3 did not significantly affect action potentials compared to PP2 effects (F). Similar results were observed in an additional five myocytes.

Figure 2A shows that PP2 (1μM, incubation for 15–30min) hyperpolarized the membrane potential and decreased the slow diastolic depolarization. For comparison, ISO (10 nM) increased diastolic depolarization (Figure 2B). These results were reproduced in an additional 6 cells.

Since the cardiac pacemaker "funny" current, I_f, is the depolarizing current that contributes to sinus node diastolic depolarization (11), we next examined PP2 effects on I_f.

PP2 decreased rat sinus node I_f

Figure 3A shows a representative I_f recorded in an isolated rat sinus node myocyte. The inset shows that the current is relatively insensitive to 2 mM Ba^{2+}, but can be blocked by 1 mMCs^+ or 2 μM ZD7288, which are typical characteristics of I_f (11). The activation threshold (V_{th}, the voltage at which the first time-dependent inward current larger than 10 pA was detected) and midpoint ($V_{1/2}$, the voltage at which the tail current amplitude reaches half activation) are −60 mV and −83 mV, respectively for this cell. The average activation midpoint is −77.8 mV (3B, Table 1). Since Ba^{2+} partially inhibited I_f (22), the activation threshold is more positive in the absence of Ba^{2+} (for example, see a supplemental figure S3).

Figure 3C shows I_f activation kinetics, which are the fastest compared to I_f in other cardiac regions such as Purkinje fibers and ventricles (23). These data demonstrate that I_f gating properties in the rat sinus node are comparable to those in sinus node of other species such as mouse (24), dog (25), human (26), and especially rabbit in which I_f has been mostly studied (12, 20).

Figure 3D shows that PP2 (2–10 μM) significantly decreased I_f measured at −100 mV (gray). The inhibition of PP2 on I_f was confirmed by recovery of the current amplitude after washout of PP2. PP3 did not inhibit I_f (gray), suggesting the inhibition of I_f by PP2 is through suppression of STK activity. In a different cell, ISO increased the current amplitude at −95 mV (3E). In the presence of PP2, however, ISO was unable to increase I_f (3E, gray). Figure 3F shows that ISO stimulation of I_f is via shifting the activation curve towards more positive voltages, an effect prevented by PP2 (3F, gray). On average, PP2 induced a hyperpolarizing shift of 10 mV in the activation midpoint of I_f, whereas ISO induced a depolarizing shift of 10.5 mV on its own and a hyperpolarizing shift of 16mV in the presence of PP2 (Table 1). The activation threshold was shifted 18.5 mV more negative by PP2, 5.6 mV more positive by ISO, and 23.5 mV more negative by PP2 and ISO together, respectively (Table 1).

The I_f activation kinetics was also slowed by PP2. On average, PP2 slowed I_f activation kinetics at −100 mV by 21%, while ISO accelerated it by 21% (Table 1). However, instead of acceleration, ISO decelerated I_f activation kinetics at −100 mV by 58% when PP2 was co-administrated (Table 1).

PP2 induced an internalization of HCN4 associated with a decreased tyrosine phosphorylation

To investigate the mechanism underlying the prevention of ISO stimulation of I_f by PP2, we explored a possible alteration of cell surface expression of HCN4 channel proteins in sinus node myocytes. Figure 4 shows the confocal fluorescent images of sinus node myocytes stained with a specific HCN4 antibody. Line scan analysis shows the different distribution patterns of fluorescence for untreated (A), PP2 treated (B), and PP3 treated cell (C). PP2 significantly decreased cell surface fluorescent signals (peaks at the edges) and increased the intracellular fluorescent signals (peaks in the middle), whereas PP3 did not.

Figure 5 shows the associated changes in tyrosine phosphorylation state of the sinus node myocytes. Compared to untreated cell (A, green), PP2 significantly decreased the tyrosine phosphorylation of the cell (B, green). In comparison, ISO increased the tyrosine phosphorylation state of the cell (C, green), and this increase was inhibited by PP2 (D, green). The altered tyrosine phosphorylation state is evidenced not only by the change in fluorescence, but also by the colocalization of HCN4 (red) and tyrosine phosphorylation state (green), shown in yellow dots marked by white arrows.

Averaging from 20 cells, PP2 reduced HCN4 channel surface expression normalized to the cell size by 37%, associated with a reduced tyrosine phosphorylation state of cells by 36% (Figure 6, open bar). ISO increased the surface expression by 54% and the tyrosine phosphorylation by 49%, respectively (Figure 6, light gray bar). The ISO-induced effects were inhibited by PP2, the surface expression and tyrosine phosphorylation were reduced by 31% and 47%, respectively (Figure 6, dark gray bar).

PP2 inhibited HCN4 and prevented the enhancement of HCN4 by ISO

PP2 suppression of HCN4 surface expression can explain PP2 prevention of ISO stimulation of I_f. To confirm this conclusion, we needed to provide direct evidence for a well-established ISO stimulation of HCN4 that is inhibited by PP2.

Figure 7 shows that the HCN4 current (A) was inhibited by PP2 (10 μM) (B) via a negative shift of activation threshold (gray line). In the presence of PP2, ISO (0.1 μM) was unable to induce a positive shift of HCN4 activation (C) in contrast to ISO stimulation of HCN4 (supplemental Figure S4 (A–C)). After PP2 washout, ISO was able to shift the HCN4 activation to more depolarizing voltages (D). On average, the activation threshold of HCN4 was positively shifted by 7.6 mV by ISO, and negatively shifted by 11.6 mV by PP2 and 16.6 mV by PP2+ISO, respectively (Table 2). The validation of the β-adrenergic signaling pathway in HEK293 cells (27) is shown in Figure S4 (B, D) and in Table 2.

Besides activation threshold, the activation midpoint of HCN4 was also shifted by PP2. The HCN4 tail current corresponding to activation at −90 mV (gray line) was near half activation (7E). PP2 negatively shifted the activation midpoint close to −100 mV (7F). In the presence of PP2, ISO was unable to positively shift the activation midpoint (7G). After PP2 washout, ISO succeeded in shifting the activation midpoint towards −80 mV (7H). The averaged activation midpoint was positively shifted by 4.9 mV by ISO, and negatively shifted by 6.3 mV by PP2 and 13.7 mV by PP2+ISO, respectively (Table 2). PP2 also slowed HCN4

activation kinetics regardless of ISO. At −120 mV, ISO accelerated the activation kinetics by 44% on average, and PP2 decelerated the activation kinetics by 67% by itself, and by 29% in the presence of ISO (Table 2).

PP2 inhibited and ISO did not affect 573x

PP2 attenuated ISO stimulation of I_f and HCN4 raised a question that PP2 may act independently of cAMP mechanism. To address this question, we examined the effects of PP2 on 573x, an HCN4 mutant that contains the C-linker but lacks the CNBD and cAMP sensitivity (28).

Figure 8 shows that PP2 inhibited 573x by shifting its activation threshold (gray line) from −65mV (8A) to −75mV (8B), which was reversible after PP2 washout (8C). The average activation threshold of 573x was negatively shifted by 18.3 mV by PP2 (V_{th}_control: −55.0 ± 2.9 mV, V_{th}_PP2: −73.3 ± 3.1 mV, n = 8). The activation midpoint was also negatively shifted by PP2 ($V_{1/2}$_control: −81.7 ± 4.3 mV, $V_{1/2}$_PP2: −92.7 ± 4.8 mV, n = 6). In addition, at −125 mV, PP2 slowed the activation kinetics of 573x by 75% (τ-act_control: 1286 ± 216 ms, τ-act_PP2: 2260 ± 268 ms, n = 6).

On the other hand, ISO exerted little effects on 573x current expression shown in Fig. 8D. This result confirms that the main target region for cAMP-mediated ISO stimulation of HCN4 channel activity is indeed CNBD that is missing in 573x.

DISCUSSION

Many inhibitors of tyrosine kinases in cancer therapy have been demonstrated to cause long QT by altering the properties of multiple ion channels (29). Long QT is often associated with bradycardia, especially in severe bradycardia caused by defective channel gating (30–32). In this work, we presented evidence for inhibition and attenuation of β-adrenergic stimulation of cardiac pacemaker activity induced by PP2, a widely used and presumably selective inhibitor of STK.

In dissected sinus node, PP2 slowed the spontaneous beating rate and blunted ISO-induced increase of beating rate (Figure S2). In isolated sinus node myocytes the number of spontaneous action potentials was dramatically reduced by PP2 (Figure 1B). The PP2-induced suppression is largely due to a hyperpolarized membrane potential and a decreased diastolic depolarization.

One important ionic current that controls the heart rate is I_f in the sinus node (11). Increased I_f depolarizes, while decreased I_f hyperpolarizes, the membrane potential (11). PP2-induced a membrane hyperpolarization, suggesting that I_f may be affected. Indeed, PP2 decreased I_f current amplitude, slowed I_f activation kinetics, and shifted I_f activation curve to more negative potentials. Further, stimulation of I_f by ISO was completely lost in the presence of PP2.

It is noted that in isolated rat sinus node myocytes, the activation threshold of I_f is well within the early diastolic depolarization of the action potential. The maximal diastolic depolarization is close to −60 mV (Figure 2), and the average I_f activation threshold is

around −50 mV in the absence of Ba^{2+} (Figure S3). To initiate the early diastolic depolarization, only a small I_f (about 1 pA) is needed due to the high membrane resistance in the sinus node cells (10).

To understand PP2 inhibition of I_f, independent of β-adrenergic stimulation, we examined the cell surface expression of HCN4, which is regulated by dynamic forward trafficking and internalization of the channel proteins (33). Due to the small size of sinus node, we chose to use confocal immunofluorescence imaging, rather than the conventional biotinylation method (16, 17), which require a much large quantity of tissue to generate sufficient amount of proteins (see details in Supplement).

Altered fluorescence distribution toward middle from the edges of cell induced by PP2 (4B) can be reasonably explained by a decreased expression at cell surface and an increased retention in the cytoplasm of HCN4 channels. This approach has been successfully used to investigate the surface expression of Cav1.2 channels (34).

We previously found a time-dependent PP2-induced decrease in tyrosine phosphorylation of HCN4 channel proteins in HEK293 (5). PP2 at 10μM can nearly abolish the tyrosine phosphorylation of HCN4 after 30min incubation. In this work, we showed that PP2 significantly reduced tyrosine phosphorylation of HCN4 in isolated sinus node myocytes (4B, green, compared to 4A, green). Furthermore, this reduced tyrosine phosphorylation is associated with a decreased surface expression of HCN4 channels.

Our previous study showed PP2 inhibition of HCN4 activity by shifting its activation curve to more negative potentials (5). In the present work, we showed that PP2 can also negatively shift 573x activation, indicating that PP2 effects on HCN4 is not mediated by CNBD and thus, independent of cAMP signaling. This conclusion is further supported by the lack of ISO effects on 573x.

These results are in agreement with the previous findings that the main sites (Y531 and Y554) that mediate STK enhancement of HCN4 are located in the C-linker, excluding the CNBD and the distal C-terminal region (5, 18).

How does PP2 attenuate ISO stimulation of cardiac pacemaker activity? Src has been identified as a direct target of $G\alpha_s$ and $G\alpha_i$ subunits (35, 36). The $G\alpha_s$ and $G\alpha_i$ subunits bind to the catalytic domain and change the conformation of c-Src *in vivo*, leading to its activation. More recently, Src has been found to be bound with and directly activated by β2 adrenergic receptors (β2AR) (37, 38). In the sinus node, β2AR is the dominant isoform that mediates the modulation of heart rate (39). These findings implicated that upon activation of β2AR, more active Src may be produced to act on HCN4 channels. This may explain a larger PP2 suppression of I_f in the presence of ISO (Table 1).

The diminished stimulation by ISO in the presence of PP2 on I_{HCN4}, sinus node I_f, action potentials, and spontaneous beating rate, respectively, supported the hypothesis that ISO can increase the sinus node pacemaker activity via a cAMP-independent, Src-mediated stimulation of HCN4 activity by phosphorylation on tentative tyrosine residues in the C-linker of the channel protein.

Recently, PP2 has been found to inhibit many other tyrosine kinases, in addition to STK (40). The PP2-induced reduction of tyrosine kinase activity from other tyrosine kinases cannot be excluded in the interpretation of the results presented in this work. Nevertheless, our results demonstrated that PP2, a widely used STK inhibitor, can decrease and attenuate the potential β-adrenergic stimulation of the spontaneous cardiac pacemaker activity, possibly via a decreased tyrosine phosphorylation of HCN4 channel proteins and channel internalization.

Finally, it is imperative to emphasize that Src tyrosine kinases have multiple targets. Src is a key modulator for PKA activation (41, 42). Thus, inhibited Src activity can result in a decreased cAMP production. Src can also directly bind to and modulate many other voltage-gated ion channels such as K^+ channel (43, 44), Na^+ channel (6), L-type Ca^{2+} channel (45, 46), and Na^+/K^+ pump (47). All these channels and pump, particularly L-type Ca^{2+} channel, can contribute to cardiac pacemaker activity (48). The critical role of Cav1.3 L-type calcium current in sinus node pacemaker activity has been well documented in rabbit (49), mouse (50–54) and human (55). Recently, another important component of cardiac pacing mechanism, "Ca^{2+} Clock", has been demonstrated to couple HCN/I_f component for cardiac pacing under physiological conditions, and particularly under β-adrenergic stimulation (56). This mechanism provides reasonable explanation for the preservation of isoproterenol stimulation of heart rate in conditional HCN4 knockout (57) and cAMP-insensitive HCN4 mutant knockin mice (14). Potential effects of PP2 on L-type calcium current and ryanodine-receptor dependent Ca^{2+} release will be the next important research question as how the inhibited Src tyrosine kinases may interfere with the modulation of "Ca^{2+} Clock" by β-adrenergic stimulation.

Supplementary Material

Refer to Web version on PubMed Central for supplementary material.

Acknowledgments

Source of support that require acknowledgement:

The plasmid, HCN4-573x is a generous gift from Dr. Dirk Isbrandt (University Medical Center Hamburg).

Disclosure of funding received for this work:

This work was supported by National Heart, Lung, and Blood Institute (HL075023) American Heart Association Grant-in-Aid (13GRNT16420018), and by the Office of Research and Graduate Programs/Health Sciences Center at West Virginia University. Jianying Huang is the recipient of an American Heart Association Predoctoral Fellowship. Microscope experiments and image analysis were performed in the West Virginia University Microscope Imaging Facility, supported in part by the Mary Babb Randolph Cancer Center and NIH Grant P20 RR016440.

References

1. Barr VA, Lane K, Taylor SI. Subcellular localization and internalization of the four human leptin receptor isoforms. J Biol Chem. 1999 Jul 23; 274(30):21416–24. [PubMed: 10409704]
2. Thomas SM, Brugge JS. Cellular functions regulated by Src family kinases. Annu Rev Cell Dev Biol. 1997; 13:513–609. [PubMed: 9442882]

3. Martin GS. The hunting of the Src. Nat Rev Mol Cell Biol. 2001 Jun; 2(6):467–75. [PubMed: 11389470]
4. Shi Y, Yadav VK, Suda N, Liu XS, Guo XE, Myers MG Jr, Karsenty G. Dissociation of the neuronal regulation of bone mass and energy metabolism by leptin in vivo. Proc Natl Acad Sci U S A. 2008 Dec 23; 105(51):20529–33. [PubMed: 19074282]
5. Li CH, Zhang Q, Teng B, Mustafa SJ, Huang JY, Yu HG. Src tyrosine kinase alters gating of hyperpolarization-activated HCN4 pacemaker channel through Tyr531. Am J Physiol Cell Physiol. 2008 Jan; 294(1):C355–62. [PubMed: 17977941]
6. Ahern CA, Zhang JF, Wookalis MJ, Horn R. Modulation of the cardiac sodium channel NaV1.5 by Fyn, a Src family tyrosine kinase. Circ Res. 2005 May 13; 96(9):991–8. [PubMed: 15831816]
7. Callera GE, Montezano AC, Yogi A, Tostes RC, He Y, Schiffrin EL, Touyz RM. c-Src-dependent nongenomic signaling responses to aldosterone are increased in vascular myocytes from spontaneously hypertensive rats. Hypertension. 2005 Oct; 46(4):1032–8. [PubMed: 16157790]
8. Heida NM, Leifheit-Nestler M, Schroeter MR, Muller JP, Cheng IF, Henkel S, Limbourg A, Limbourg FP, Alves F, Quigley JP, Ruggeri ZM, Hasenfuss G, Konstantinides S, Schafer K. Leptin enhances the potency of circulating angiogenic cells via src kinase and integrin (alpha)vbeta5: implications for angiogenesis in human obesity. Arterioscler Thromb Vasc Biol. 2010 Feb; 30(2): 200–6. [PubMed: 19910644]
9. Hanke JH, Gardner JP, Dow RL, Changelian PS, Brissette WH, Weringer EJ, Pollok BA, Connelly PA. Discovery of a novel, potent, and Src family-selective tyrosine kinase inhibitor. Study of Lck- and FynT-dependent T cell activation. J Biol Chem. 1996 Jan 12; 271(2):695–701. [PubMed: 8557675]
10. Vassalle, M.; Yu, H.; Cohen, IS. Pacemaker Channels and Cardiac Automaticity. In: Zipes, DP.; Jalife, J., editors. Cardiac Electrophysiology: From Cell to Bedside. 3. W.B. Saunders Company; 1999. p. 94-103.
11. DiFrancesco D. The role of the funny current in pacemaker activity. Circ Res. 2010 Feb 19; 106(3):434–46. [PubMed: 20167941]
12. Shi W, Wymore R, Yu H, Wu J, Wymore RT, Pan Z, Robinson RB, Dixon JE, McKinnon D, Cohen IS. Distribution and prevalence of hyperpolarization-activated cation channel (HCN) mRNA expression in cardiac tissues. Circ Res. 1999 Jul 9; 85(1):e1–6. [PubMed: 10400919]
13. Wainger BJ, DeGennaro M, Santoro B, Siegelbaum SA, Tibbs GR. Molecular mechanism of cAMP modulation of HCN pacemaker channels. Nature. 2001 Jun 14; 411(6839):805–10. [PubMed: 11459060]
14. Alig J, Marger L, Mesirca P, Ehmke H, Mangoni ME, Isbrandt D. Control of heart rate by cAMP sensitivity of HCN channels. Proceedings of the National Academy of Sciences. Jul 21; 2009 106(29):12189–94.
15. Arinsburg SS, Cohen IS, Yu HG. Constitutively active Src tyrosine kinase changes gating of HCN4 channels through direct binding to the channel proteins. J Cardiovasc Pharmacol. 2006 Apr; 47(4):578–86. [PubMed: 16680072]
16. Huang J, Huang A, Zhang Q, Lin YC, Yu HG. Novel Mechanism for Suppression of Hyperpolarization-activated Cyclic Nucleotide-gated Pacemaker Channels by Receptor-like Tyrosine Phosphatase-{alpha}. J Biol Chem. 2008 Oct 31; 283(44):29912–9. [PubMed: 18768480]
17. Lin Y-C, Huang J, Kan H, Frisbee JC, Yu H-G. Rescue of a trafficking defective human pacemaker channel via a novel mechanism: roles of Src, Fyn, Yes tyrosine kinases. J Biol Chem 2009. Sep 11.2009 284:30433–40.
18. Zong X, Eckert C, Yuan H, Wahl-Schott C, Abicht H, Fang L, Li R, Mistrik P, Gerstner A, Much B, Baumann L, Michalakis S, Zeng R, Chen Z, Biel M. A novel mechanism of modulation of hyperpolarization-activated cyclic nucleotide-gated channels by Src kinase. J Biol Chem. 2005 Oct 7; 280(40):34224–32. [PubMed: 16079136]
19. Shinagawa Y, Satoh H, Noma A. The sustained inward current and inward rectifier K+ current in pacemaker cells dissociated from rat sinoatrial node. The Journal of Physiology. Mar 15; 2000 523(3):593–605. [PubMed: 10718740]

20. Wu JY, Yu H, Cohen IS. Epidermal growth factor increases i(f) in rabbit SA node cells by activating a tyrosine kinase. Biochim Biophys Acta. 2000 Jan 15; 1463(1):15–9. [PubMed: 10631290]
21. Bain J, McLauchlan H, Elliott M, Cohen P. The specificities of protein kinase inhibitors: an update. Biochem J. 2003 Apr 1; 371(Pt 1):199–204. [PubMed: 12534346]
22. DiFrancesco D, Ferroni A, Mazzanti M, Tromba C. Properties of the hyperpolarizing-activated current (if) in cells isolated from the rabbit sino-atrial node. J Physiol. 1986 Aug.377:61–88. [PubMed: 2432247]
23. Yu H, Chang F, Cohen IS. Pacemaker current i(f) in adult canine cardiac ventricular myocytes. J Physiol. 1995 Jun 1; 485(Pt 2):469–83. [PubMed: 7545232]
24. Cho H-S, Takano M, Noma A. The electrophysiological properties of spontaneously beating pacemaker cells isolated from mouse sinoatrial node. The Journal of Physiology. Jul 1; 2003 550(1):169–80. [PubMed: 12879867]
25. Gao Z, Chen B, Joiner ML, Wu Y, Guan X, Koval OM, Chaudhary AK, Cunha SR, Mohler PJ, Martins JB, Song LS, Anderson ME. I(f) and SR Ca(2+) release both contribute to pacemaker activity in canine sinoatrial node cells. J Mol Cell Cardiol. 2010 Jul; 49(1):33–40. [PubMed: 20380837]
26. Verkerk AO, Wilders R, van Borren MM, Peters RJ, Broekhuis E, Lam K, Coronel R, de Bakker JM, Tan HL. Pacemaker current (If) in the human sinoatrial node. Eur Heart J. 2007 Oct; 28(20): 2472–8. [PubMed: 17823213]
27. Friedman J, Babu B, Clark RB. β2-Adrenergic Receptor Lacking the Cyclic AMP-Dependent Protein Kinase Consensus Sites Fully Activates Extracellular Signal-Regulated Kinase 1/2 in Human Embryonic Kidney 293 Cells: Lack of Evidence for Gs/Gi Switching. Molecular Pharmacology. Nov 1; 2002 62(5):1094–102. [PubMed: 12391272]
28. Schulze-Bahr E, Neu A, Friederich P, Kaupp UB, Breithardt G, Pongs O, Isbrandt D. Pacemaker channel dysfunction in a patient with sinus node disease. J Clin Invest. 2003 May; 111(10):1537–45. [PubMed: 12750403]
29. Lu Z, Wu CY, Jiang YP, Ballou LM, Clausen C, Cohen IS, Lin RZ. Suppression of phosphoinositide 3-kinase signaling and alteration of multiple ion currents in drug-induced long QT syndrome. Sci Transl Med. 2012 Apr 25.4(131):131ra50.
30. Ueda K, Nakamura K, Hayashi T, Inagaki N, Takahashi M, Arimura T, Morita H, Higashiuesato Y, Hirano Y, Yasunami M, Takishita S, Yamashina A, Ohe T, Sunamori M, Hiraoka M, Kimura A. Functional characterization of a trafficking-defective HCN4 mutation, D553N, associated with cardiac arrhythmia. J Biol Chem. 2004 Jun 25; 279(26):27194–8. [PubMed: 15123648]
31. Bence-Hanulec KK, Marshall J, Blair LAC. Potentiation of Neuronal L Calcium Channels by IGF-1 Requires Phosphorylation of the ±1 Subunit on a Specific Tyrosine Residue. Neuron. 2000; 27(1):121–31. [PubMed: 10939336]
32. Banks AS, Davis SM, Bates SH, Myers MG Jr. Activation of downstream signals by the long form of the leptin receptor. J Biol Chem. 2000 May 12; 275(19):14563–72. [PubMed: 10799542]
33. Hardel N, Harmel N, Zolles G, Fakler B, Klocker N. Recycling endosomes supply cardiac pacemaker channels for regulated surface expression. Cardiovasc Res. 2008 Jul 1; 79(1):52–60. [PubMed: 18326556]
34. Wang HG, George MS, Kim J, Wang C, Pitt GS. Ca2+/calmodulin regulates trafficking of Ca(V)1.2 Ca2+ channels in cultured hippocampal neurons. J Neurosci. 2007 Aug 22; 27(34): 9086–93. [PubMed: 17715345]
35. Luttrell LM, Hawes BE, van Biesen T, Luttrell DK, Lansing TJ, Lefkowitz RJ. Role of c-Src Tyrosine Kinase in G Protein-coupled Receptorand Gβγ Subunit-mediated Activation of Mitogen-activated Protein Kinases. Journal of Biological Chemistry. Aug 9; 1996 271(32):19443–50. [PubMed: 8702633]
36. Ma YC, Huang J, Ali S, Lowry W, Huang XY. Src tyrosine kinase is a novel direct effector of G proteins. Cell. 2000 Sep 1; 102(5):635–46. [PubMed: 11007482]
37. Sun Y, Huang J, Xiang Y, Bastepe M, Juppner H, Kobilka BK, Zhang JJ, Huang X-Y. Dosage-dependent switch from G protein-coupled to G protein-independent signaling by a GPCR. EMBO J. 2007; 26(1):53–64. [PubMed: 17170700]

38. Fan, G-f; Shumay, E.; Malbon, CC.; Wang, H-y. c-Src Tyrosine Kinase Binds the β2-Adrenergic Receptor via Phospho-Tyr-350, Phosphorylates G-protein-linked Receptor Kinase 2, and Mediates Agonist-induced Receptor Desensitization. Journal of Biological Chemistry. Apr 20; 2001 276(16):13240–7. [PubMed: 11278940]
39. Barbuti A, Terragni B, Brioschi C, DiFrancesco D. Localization of f-channels to caveolae mediates specific beta2-adrenergic receptor modulation of rate in sinoatrial myocytes. J Mol Cell Cardiol. 2007 Jan; 42(1):71–8. [PubMed: 17070839]
40. Brandvold KR, Steffey ME, Fox CC, Soellner MB. Development of a highly selective c-Src kinase inhibitor. ACS Chem Biol. 2012 Aug 17; 7(8):1393–8. [PubMed: 22594480]
41. Abrahamsen H, Vang T, Tasken K. Protein kinase A intersects SRC signaling in membrane microdomains. J Biol Chem. 2003 May 9; 278(19):17170–7. [PubMed: 12606547]
42. Baker MA, Hetherington L, Aitken RJ. Identification of SRC as a key PKA-stimulated tyrosine kinase involved in the capacitation-associated hyperactivation of murine spermatozoa. J Cell Sci. 2006 Aug 1; 119(Pt 15):3182–92. [PubMed: 16835269]
43. Holmes TC, Fadool DA, Ren R, Levitan IB. Association of Src Tyrosine Kinase with a Human Potassium Channel Mediated by SH3 Domain. Science. Dec 20; 1996 274(5295):2089–91. [PubMed: 8953041]
44. Gamper N, Stockand JD, Shapiro MS. Subunit-specific modulation of KCNQ potassium channels by Src tyrosine kinase. J Neurosci. 2003 Jan 1; 23(1):84–95. [PubMed: 12514204]
45. Dubuis E, Rockliffe N, Hussain M, Boyett M, Wray D, Gawler D. Evidence for multiple Src binding sites on the alpha1c L-type Ca2+ channel and their roles in activity regulation. Cardiovasc Res. 2006 Feb 1; 69(2):391–401. [PubMed: 16352297]
46. Kang M, Ross GR, Akbarali HI. COOH-terminal association of human smooth muscle calcium channel Ca(v)1.2b with Src kinase protein binding domains: effect of nitrotyrosylation. Am J Physiol Cell Physiol. 2007 Dec; 293(6):C1983–90. [PubMed: 17942635]
47. Tian J, Cai T, Yuan Z, Wang H, Liu L, Haas M, Maksimova E, Huang XY, Xie ZJ. Binding of Src to Na+/K+-ATPase forms a functional signaling complex. Mol Biol Cell. 2006 Jan; 17(1):317–26. [PubMed: 16267270]
48. Irisawa H, Brown HF, Giles W. Cardiac pacemaking in the sinoatrial node. Physiol Rev. 1993 Jan; 73(1):197–227. [PubMed: 8380502]
49. Verheijck EE, van Ginneken AC, Wilders R, Bouman LN. Contribution of L-type Ca2+ current to electrical activity in sinoatrial nodal myocytes of rabbits. Am J Physiol. 1999 Mar; 276(3 Pt 2):H1064–77. [PubMed: 10070093]
50. Platzer J, Engel J, Schrott-Fischer A, Stephan K, Bova S, Chen H, Zheng H, Striessnig J. Congenital deafness and sinoatrial node dysfunction in mice lacking class D L-type Ca2+ channels. Cell. 2000 Jul 7; 102(1):89–97. [PubMed: 10929716]
51. Zhang Z, Xu Y, Song H, Rodriguez J, Tuteja D, Namkung Y, Shin HS, Chiamvimonvat N. Functional Roles of Ca(v)1.3 (alpha(1D)) calcium channel in sinoatrial nodes: insight gained using gene-targeted null mutant mice. Circ Res. 2002 May 17; 90(9):981–7. [PubMed: 12016264]
52. Mangoni ME, Couette B, Bourinet E, Platzer J, Reimer D, Striessnig J, Nargeot J. Functional role of L-type Cav1.3 Ca2+ channels in cardiac pacemaker activity. Proc Natl Acad Sci U S A. 2003 Apr 29; 100(9):5543–8. [PubMed: 12700358]
53. Mangoni ME, Couette B, Marger L, Bourinet E, Striessnig J, Nargeot J. Voltage-dependent calcium channels and cardiac pacemaker activity: from ionic currents to genes. Prog Biophys Mol Biol. 2006 Jan-Apr;90(1–3):38–63. [PubMed: 15979127]
54. Mangoni ME, Nargeot J. Genesis and regulation of the heart automaticity. Physiol Rev. 2008 Jul; 88(3):919–82. [PubMed: 18626064]
55. Baig SM, Koschak A, Lieb A, Gebhart M, Dafinger C, Nurnberg G, Ali A, Ahmad I, Sinnegger-Brauns MJ, Brandt N, Engel J, Mangoni ME, Farooq M, Khan HU, Nurnberg P, Striessnig J, Bolz HJ. Loss of Ca(v)1.3 (CACNA1D) function in a human channelopathy with bradycardia and congenital deafness. Nat Neurosci. 2011 Jan; 14(1):77–84. [PubMed: 21131953]
56. Lakatta EG, Maltsev VA, Vinogradova TM. A coupled SYSTEM of intracellular Ca2+ clocks and surface membrane voltage clocks controls the timekeeping mechanism of the heart's pacemaker. Circ Res. 2010 Mar 5; 106(4):659–73. [PubMed: 20203315]

57. Baruscotti M, Bucchi A, Viscomi C, Mandelli G, Consalez G, Gnecchi-Rusconi T, Montano N, Casali KR, Micheloni S, Barbuti A, DiFrancesco D. Deep bradycardia and heart block caused by inducible cardiac-specific knockout of the pacemaker channel gene Hcn4. Proc Natl Acad Sci U S A. 2011 Jan 25; 108(4):1705–10. [PubMed: 21220308]

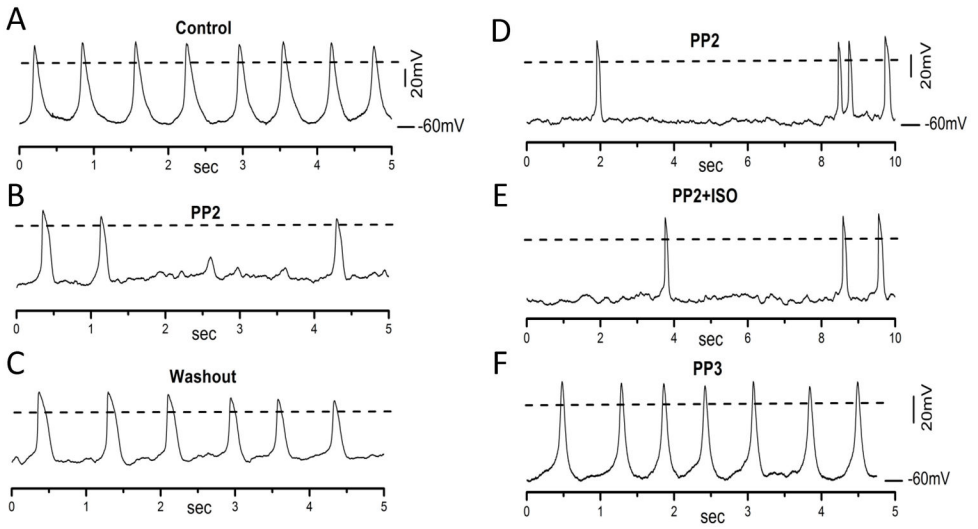

Figure 1. PP2 slows and prevents ISO stimulation of action potentials in isolated sinus node myocytes

(A) spontaneous action potentials (APs) recorded from a sinus node myocyte. (B) PP2 at 2 μM reduced the number of APs that were spontaneously fired. (C) Washout of PP2 partially recovered the number of APs. Similar experiments were repeated in an additional 4 cells. Dash lines indicate 0mV. (D) APs recorded from a different sinus node myocyte pretreated with 2 μM PP2 for 2–4 min. (E) In the presence of PP2, ISO (10 nM) failed to increase the number of APs. Similar experiments were repeated in an additional 3 cells. (F) APs recorded from a different myocyte incubated with PP3 (2 μM) for 5 min. Similar results were obtained in an additional 4 cells.

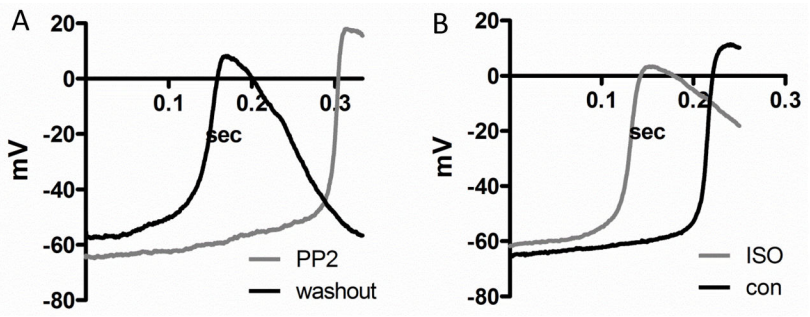

Figure 2. PP2 inhibits diastolic depolarization in isolated sinus node myocytes

(A) action potentials were recorded in the same cell incubated with PP2 (1μM, 15–30min) (gray) and washout (black). Removal of PP2 depolarized membrane potential and increased the slow diastolic depolarization. (B) action potentials were recorded in the same cell in the absence and presence of 10nM ISO (grey).

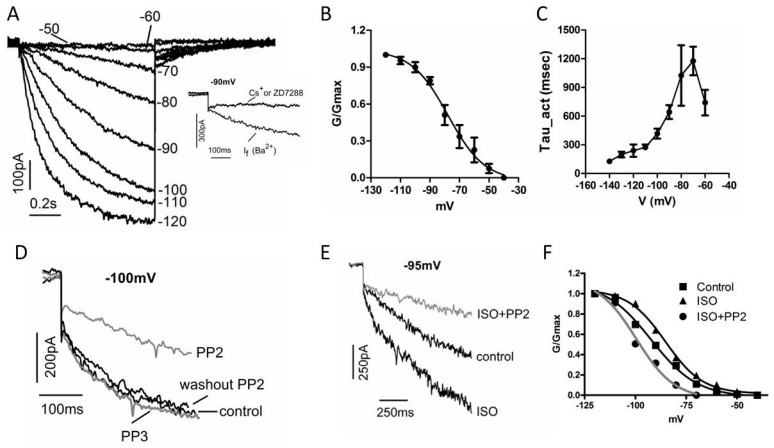

Figure 3. PP2 decreases and prevents ISO stimulation of I_f

(A) I_f currents elicited by 1-second pulses from −50 mV to −120 mV in 10 mV increments. The holding potential was −30 mV. The inset shows that I_f current was not blocked by 2 mM Ba^{2+}, but by 1 mM Cs^+ or 2 μM ZD7288. (B) I_f activation curve constructed from tail currents averaged from 7 cells. (C) I_f activation kinetics averaged from 7 cells. (D) At −100 mV**,** I_f (dark line, control) was unaffected by PP3 (gray line) but significantly decreased by PP2 (gray line). Washout of PP2 increased I_f (dark line). (E) At −95 mV, I_f (control) was increased by ISO, but decreased in the presence of ISO and PP2 (gray line). (F) activation curves for I_f (Control), in response to ISO and ISO+PP2 (gray line), respectively.

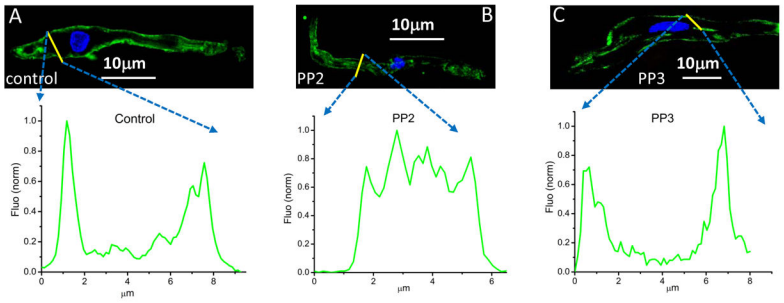

Figure 4. PP2 induces HCN4 internalization in isolated sinus node myocytes

Cross-sectional images showing isolated sinus node myocytes untreated (A) and treated with 10 μM PP2 for 10 min (B), and treated with 10 μM PP3 for 10min (C). The histogram of fluorescence corresponding to each condition is shown below the respective image. (A) In control, most HCN4 channels are expressed at the surface. (B) PP2 treatment results in intensive internalization of HCN4 channels, (C) while PP3 did not affect the surface expression of HCN4 channels. Blue: DAPI. The similar results were observed in an additional 7–11 myocytes.

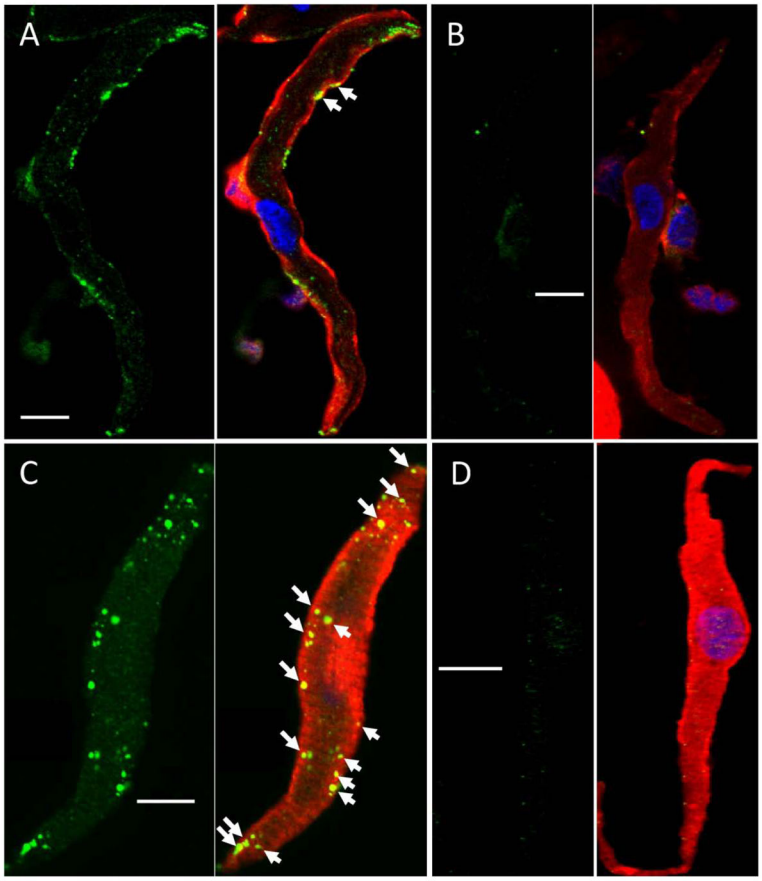

Figure 5. PP2 reduces the tyrosine phosphorylation of HCN4 in isolated sinus node myocytes

(A) untreated cell, (B) PP2 (10 μM) treated for 10 min, (C) ISO (0.1 μM) treated for 10 min, (D) ISO (0.1 μM) + PP2 (10 μM) treated for 10 min. Tyrosine phosphorylation of HCN4 channel is indicated by colocalization (yellow spots marked by white arrows) of HCN4 (red) andphosphotyrosine (green) fluorescent signals. Scale bar: 10 μm. Blue: DAPI. The similar results were observed in an additional 6–9 myocytes.

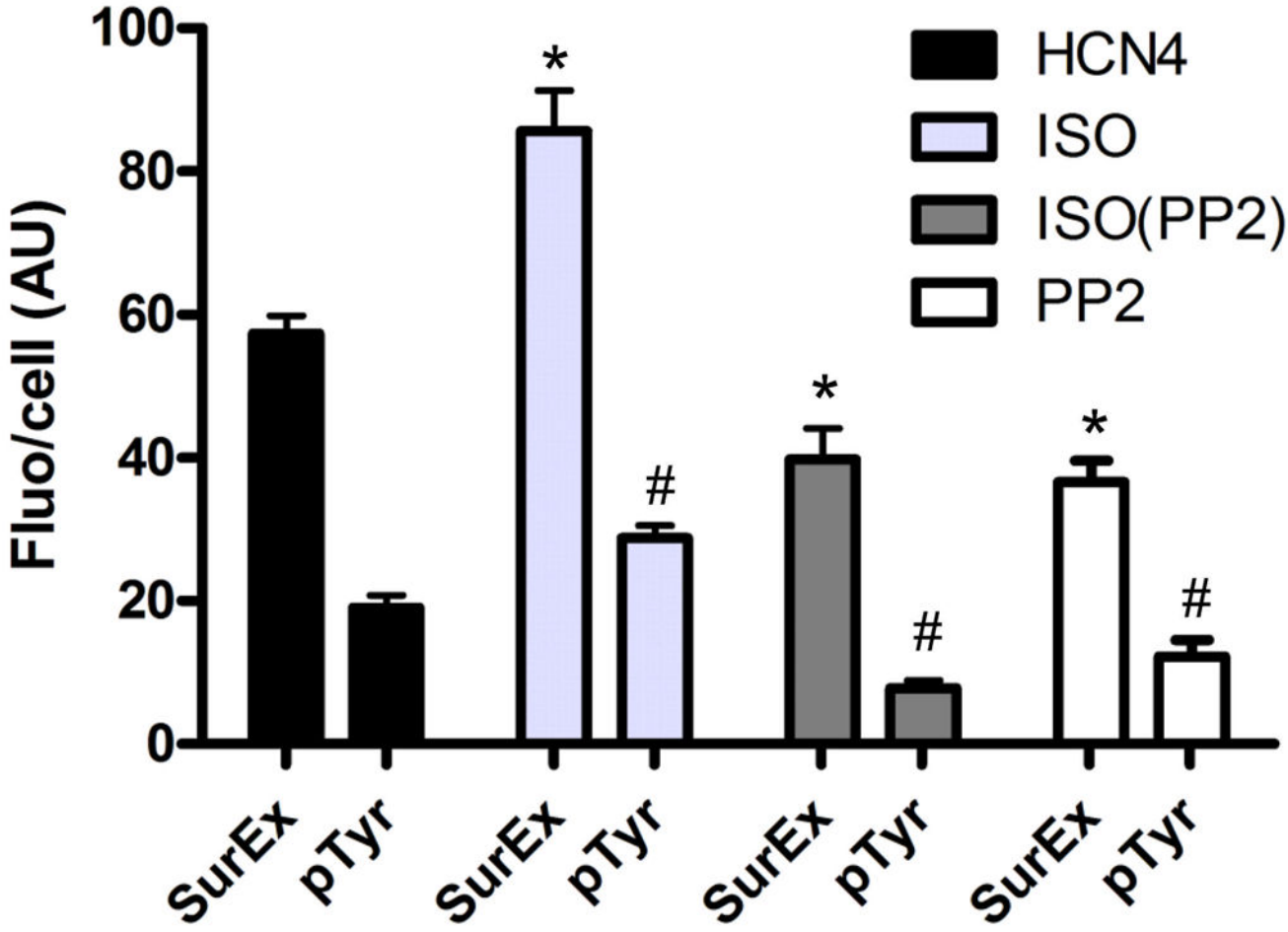

Figure 6. Average inhibition of PP2 on surface expression and tyrosine phosphorylation of HCN4 in sinus node myocytes

Fluorescence signals for HCN4 surface fluorescence and tyrosine phosphorylation normalized to cell are represented in arbitrary unit (AU). ISO's effects are shown in light grey bars. PP2's effects are shown in open bars. PP2's effects in the presence of ISO are shown in dark grey bars. The average results were from fluorescence analysis in 20 myocytes. * indicates statistically significant difference on surface expression compared to untreated myocytes. # indicates statistically significant difference on tyrosine phosphorylation state compared to untreated myocytes.

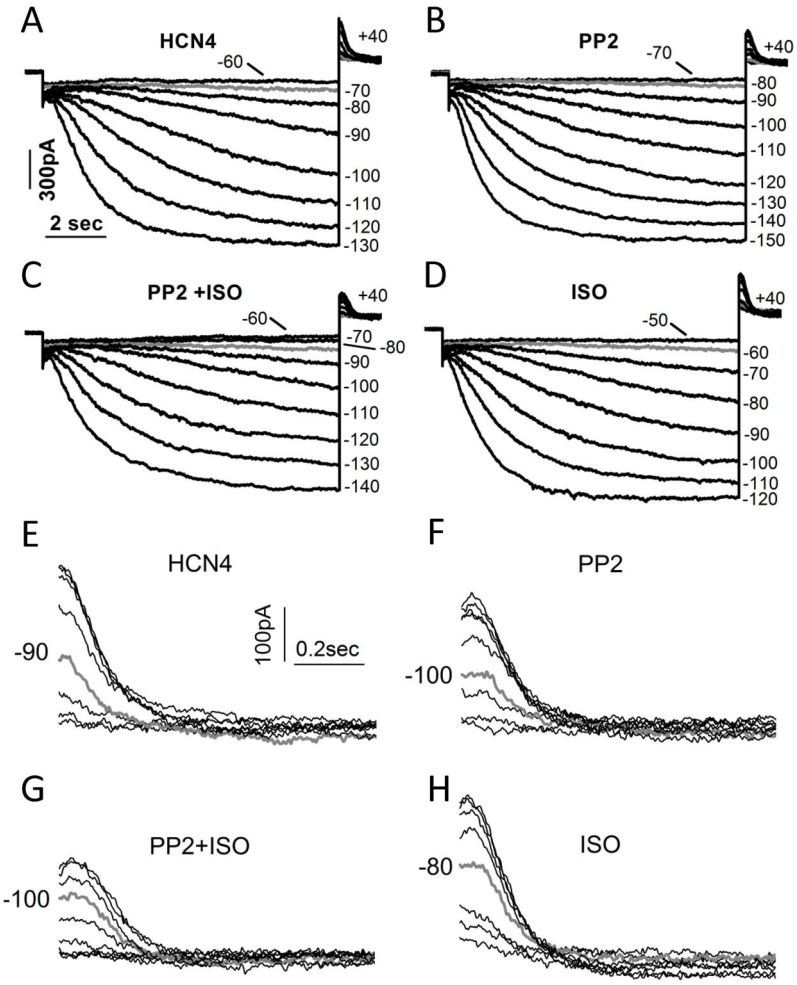

Figure 7. PP2 prevents enhancement of HCN4 by ISO

(A) HCN4 currents in a HEK293 cell elicited by 10-sec hyperpolarizing pulses as indicated. (B) HCN4 currents in the presence of PP2. (C) HCN4 currents in the presence of PP2 and ISO. (D) HCN4 currents in the presence of ISO alone after washout of PP2. (E) Enlarged HCN4 tails from A. (F) Enlarged HCN4 tails from B. (G) Enlarged HCN4 tails from C. (H) Enlarged HCN4 tails from D. Current traces in gray correspond to the activation threshold (A–D) or voltages close to the activation midpoint (E–H).

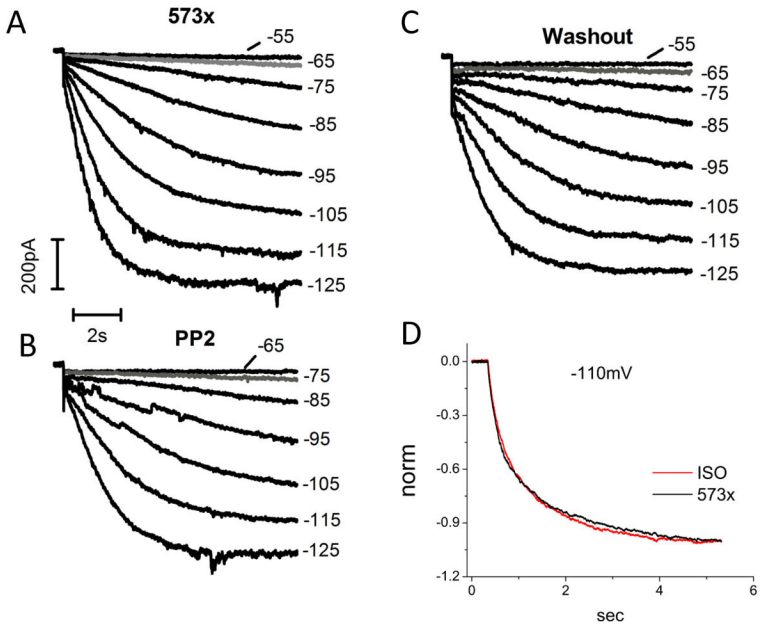

Figure 8. PP2 inhibits and ISO does not affect HCN4-573x in HEK293 cells

(A) HCN4-573c current expression in response to 10-sec hyperpolarizing pulses from −55 mV to −125 mV in 10 mV increments; (B) after 5–10 min perfusion of PP2 (10 μM); (C) after PP2 washout. Currents in gray indicate the activation threshold. (D) ISO did not affect 573x current expression. Currents were normalized for easy comparison of current traces recorded at −110mV.

Table 1

Effects of PP2 and ISO on rat sinus node I_f (Ba^{2+} in solution)

	V_{th}(mV)	$V_{1/2}$(mV)	τ-act (−100mV) (ms)
Control	−59.4±4.8(n=11)	−77.8±2.3(n=9)	416.3±20.9(n=11)
PP2*	−77.9±3.9(n=8)	−87.8±2.3(n=6)	502.3±48.1(n=6)
ISO	−53.8±4.0(n=9)	−67.3±2.3(n=7)	328.8±22.0(n=7)
ISO+PP2*	−82.9±3.6(n=6)	−93.8±1.5(n=6)	658.0±36.1(n=6)

* PP3 did not have the effects of PP2 shown in the table.

Table 2

Effects of PP2 and ISO on HCN4 gating properties

	V_{th}(mV)	$V_{1/2}$(mV)	τ-act (−120mV) (ms)
Control	−66.7±3.6(n=15)	−87.2±3.5(n=10)	2439±110(n=10)
PP2*	−78.3±2.8(n=9)	−93.5±2.9(n=7)	4075±305(n=7)
ISO	−59.1±4.4(n=7)	−82.3±2.3(n=7)	1356±127(n=7)
PP2*+ISO	−83.3±3.3(n=6)	−100.9±2.3(n=6)	3135±173(n=6)

* PP3 did not have the effects of PP2 shown in the table.